

Optical Photometrical Observations and Variability for Quasar 4C 29.45

J. H. Fan^{1,2}, J. Tao³, B. C. Qian³, A. C. Gupta⁴, Y. Liu¹,
Y. H. Yuan¹, J.H. Yang⁵, H. G. Wang¹, Y. Huang¹

¹ *Center for Astrophysics, Guangzhou University, Guangzhou 510400, China*

² *Physics Institute, Hunan Normal University, Changsha, China*

³ *Shanghai Astronomical Observatory, Chinese Academy of Sciences, Shanghai 200030, China*

⁴ *Tata Institute of Fundamental Research, Homi Bhabha Road, Colaba, Mumbai - 400 005, India*

⁵ *Department of Physics and Electronics Science, Hunan University of Arts and Science,
No. 170, West Dongting Avenue, Changde 415000, P.R.China*

(Received {reception date}); accepted {acceptation date})

Abstract

We reported the result of long term optical variability of the blazar 4C 29.45 (QSO 1156+295, Ton 599), carried out optical photometric observations in Johnson V, Cousins RI passbands during April 1997 to March 2002 using the 1.56 meter telescope of the Shanghai Astronomical Observatory (SHAO) at Sheshan, China, compiled the post-1974 optical photometric data of the blazar by combining our new observations with the published optical data, and found maximum variations in different passbands: $\Delta U = 4.41$ mag, $\Delta B = 5.55$ mag, $\Delta V = 4.53$ mag, $\Delta R = 5.80$ mag, and $\Delta I = 5.34$ mag. The average color indices are: $U-B = -0.54 \pm 0.18$ mag, $B-V = 0.56 \pm 0.21$ mag, $B-R = 0.93 \pm 0.18$ mag, $B-I = 1.51 \pm 0.24$ mag, $V-R = 0.44 \pm 0.15$ mag and $V-I = 1.03 \pm 0.23$ mag. The post-1974 data give us an excellent opportunity to search for the existence of possible periodicity in the light curve. In search for periodicity in the R passband light curve, we performed Jurkevich test and power spectral (Fourier) analysis methods, and CLEANest algorithms to remove false signals. We found possible periods of 3.55 and 1.58 years. The possible mechanism for the periodic variability was discussed.

Key words: Galaxies: active - Galaxies: photometry - Quasar:Individual: 4C 29.45 (1156+295)

1. Introduction

BL Lac objects (BLs) and flat spectrum radio quasars (FSRQs) are collectively known as blazars and belong to a subclass of radio-loud active galactic nuclei (AGNs). FSRQs include the highly polarized quasars-HPQs, the optically violently variables quasars-OVV, core-dominated quasars-CDQ, and even superluminal sources-SM. Blazars are characterized by large and violent flux variations, high and variable polarization, predominantly non-thermal emission at almost entire electromagnetic spectrum and relativistic electrons tangled with magnetic field in a relativistic jet nearly pointing towards our line of sight (see Urry & Padovani 1995 for a review). The variability time scales of blazars range from a few minutes to several years and can be broadly divided into three classes viz. micro-variability or intra-day variability (IDV), short term variability and long term variability. Time scales for micro-variability, short term variability and long term variability are a few minutes to less than a day, a few days to less than a month and months to several years respectively (Fan 2005).

Photometric observations of blazars is an important tool to construct their light curves and study the flux variation behavior on the diverse time scales. Blazars are known to show occasional, unpredicted outbursts. The origin of these outbursts is not yet well understood. It was found to be common that the light curves of blazars show

slow variations over the time scale of years (Fan 2005).

Searching for periodicity in the long term light curve of blazars is an important tool to predict and catch major outbursts. After the periodicity reported in the blazar 3C 120 (Jurkevich 1971), some other sources were also claimed to show periodicity in their light curves (e.g. Ciprini et al. 2003; Ciprini et al. 2004; Clements et al. 2003; Fan et al. 1997; Fan et al. 1998a; Fan et al. 2002; Fiorucci et al. 2004; Kidger et al. 1992; Lainela et al. 1999; Liu & Xie 1995; Manchanda 2002; Qian & Tao 2004; Raiteri et al. 2001; Sillanpää et al. 1988; Zhang et al. 1999 and reference therein). On the basis of binary black hole model given by Sillanpää et al. (1988) for the blazar OJ 287, they predicted that there should be an outburst in the blazar in the year 1994. The predicted outburst was really observed in OJ 287 in their OJ-94 project (Sillanpää et al. 1996).

To establish the reality of periods, we need long duration data. The lengthy data record required to demonstrate for periodicity depends on signal-to-noise ratio, systematic errors, regularity in times of measurements and nature of the underlying variation. Perfectly evenly sampled data on a perfectly periodic variation might not be require for more than 1.5 periods to yield an accurate measurement of the period (Fan et al. 1998a). But for most of the blazars, existing data samples do not produce evenly sampled data due to irregular telescope time allotment and sometimes cloudy sky condition in which observing

run could not be carried out. In this situation, data for a much longer time span, say six times of the period, will be useful to demonstrate the possible period. Periodicity is not simply a random event but probably has some physical significance (Kidger et al. 1992, also see Fan et al. 1997).

4C 29.45 is an OVV located at $z = 0.729$ (Wills et al. 1983; Glassgold et al. 1983; Wills et al. 1992) and has shown large variation (Branly et al. 1996), high and variable polarizations ($P_{IR} = 28.06\%$, $P_{opt} = 28\%$, Holmes et al. 1984; Mead et al. 1990) with its position angle, fraction of the optical polarization varying very dramatically (Hong et al. 1999). It has also been noticed that the source shows short and long term optical flux variability (Noble & Miller 1996; Reith & Martin 2001; Ghosh et al. 2000).

This source is one of our prime candidates for the long term monitoring in the optical pass bands from SHAO. In this paper, we presented the historical optical data of 4C 29.45 from the published literature and from our new VRI passbands observations during the period of 1997 to 2002. Section 2 presents the observations and data reduction technique, and results, in section 3 we report the data from the published literature, in section 4 the periodicity analysis, in section 5 the optical and radio correlation, in section 6 discussion and conclusions are given.

2. Observations and the data reduction

2.1. Observations

Photometric observations of 4C 29.45 were carried out in BV Johnson and RI Cousins pass bands using a liquid nitrogen cooled 200 series $1K \times 1K$ CCD detector at $f/10$ Cassegrain focus of the 1.56m telescope at SHAO, China. The each pixel of the CCD detector projected on the sky corresponds to $0.25''$ in both the dimensions. The entire CCD chip covers $\sim 4.3 \times 4.3 \text{ arcmin}^2$ on the sky. The seeing at SHAO usually varied from $1.2''$ to $1.5''$ during our observing runs. Several bias frames were taken in each observing night, sky flats were taken during twilight hours and some times dome flats were also taken.

2.2. Data reduction

For each night, median bias and median flats were generated and used for image processing (removing internal effect of the CCD detector). Image processing (bias subtraction, flat field correction and cosmic rays removal) were done by using the standard routines in the IRAF software. Processing of the data (getting instrumental magnitude of standard stars and blazar in the field of the blazar 4C 29.45) was done by multiple concentric circular aperture photometric technique using APPHOT task of the IRAF software at Guangzhou University, Guangzhou, China and at Shanghai Astronomical Observatory, Shanghai, China using Pentium 4 computers.

We have used the method of our earlier papers (Fan, Qian & Tao 2001; Qian, Tao & Fan 2004, see also Gu et al. 2006) for determining the differential magnitudes $O - S_1$, $O - S_2$ and $S_1 - S_2$ where O, S_1 and S_2 are blazar, standard star 1 and standard star 2 respectively in the

blazar field. We try to choose S_1 and S_2 of nearly similar brightness of O. In case, if we do not have S_1 and S_2 of nearly similar brightness of O, we accept $O - S_1$, $O - S_2$, and $S_1 - S_2 \leq 3 \text{ mag}$. This selection effect will not give large difference in the uncertainty determination in the $O - S_1$, $O - S_2$ and $S_1 - S_2$. When we have more than 2 standard stars in the blazar field satisfying our standard star selection criterion, we calculate the differential magnitude between these standard stars and the deviation in the differential magnitude. Finally, we select only two standard stars which have the least deviation. We investigate the variability of the blazar by using the variability parameter C introduced by Romero, Cellone & Combi (1999) (see also Cellone, Romero & Combi 2000; Fan, Qian & Tao 2001). C is expressed as

$$C = \frac{\sigma_{(O-S_1)}}{\sigma_{(S_1-S_2)}} \quad (1)$$

where $\sigma_{(O-S_1)}$ and $\sigma_{(S_1-S_2)}$ are the scatters of $O - S_1$ and $S_1 - S_2$ respectively. If $C > 3$, then the target source is variable.

The rms errors are calculated from the two standard stars using the following equation:

$$\sigma = \sqrt{\frac{\sum (m_i - \bar{m})^2}{N - 1}} \quad (2)$$

where $m_i = (m_{S_1} - m_{S_2})_i$ is the differential magnitude of stars S_1 and S_2 while $\bar{m} = \overline{m_{S_1} - m_{S_2}}$ is the differential magnitude averaged over the entire data set, and N is the number of the observations in a particular night.

Our calculations show that the $O - S_1$, $O - S_2$ and $S_1 - S_2$ for all four standard stars in the blazar 4C 29.45 field are not greater than 3 for V, R, and I band magnitudes. Therefore, we could easily select any two of these four stars (see Table 1) by using our selection criterion for standard stars discussed above for data calibration purpose. For data in V and R bands, we found star 1 and star 13 gave minimum deviation, so, we used star 1 as S_1 and star 13 as S_2 for calibrating our V and R bands data.

Since star 1 does not have I magnitude, we determined the I magnitude of the blazar in the following way. We calibrated the blazar separately by using star 13, star 14 and star 15. The calibrated I band magnitudes corresponding to star 13, star 14 and star 15 are called as m_{13}^I , m_{14}^I and m_{15}^I respectively. Final I band magnitude of the blazar is reported by using the value of $\frac{1}{3}(m_{13}^I + m_{14}^I + m_{15}^I)$ and the deviation of m_{13}^I , m_{14}^I and m_{15}^I as the uncertainty of the magnitude. This method is also used to determine the magnitude and the magnitude uncertainty of the blazar when there were ≤ 2 sets of the observations present in a single night.

2.3. Observation results

The results of our photometric observations of 4C 29.45 during January 1998 to March 2002 in V and R bands, April 1997 to March 2002 in I band are given in Table 2 and plotted in Fig. 1. Column 1 in Table 2 gives the Julian date, columns 2, 4, 6 represent V, R, I magnitudes respectively, columns 3, 5, 7 give the uncertainty in V,

Table 1. Standard stars name and magnitude in the field of the blazar 4C 29.45. In the last column of the table, 1 and 2 refer Raiteri et al. (1998) and Smith et al. (1995) respectively.

Star Name	V mag	R mag	I mag	Ref.
Star 1	13.39±0.05	13.01±0.02		1
Star 13	15.36±0.04	14.97±0.04	14.62±0.07	2
Star 14	15.89±0.09	15.53±0.08	15.16±0.18	2
Star 15	16.60±0.05	16.30±0.04	15.88±0.30	2

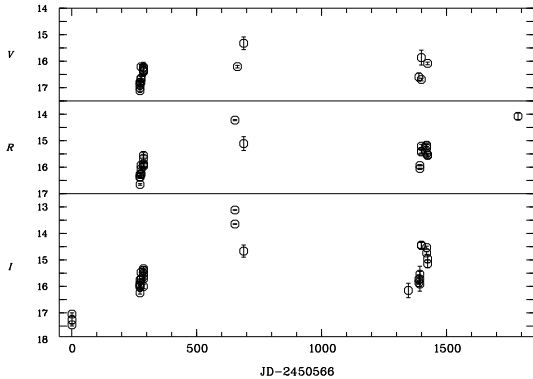


Fig. 1. Light curves of 4C 29.45. The upper panel is for V from 1998 to 2002, the middle panel is for R from 1998 to 2002, and the bottom panel is for I from 1997 to 2002 respectively.

R, I data respectively. The light curves clearly show the violent variability behavior of the source. We found large variations (e.g. 2.08 mag (15.32 to 17.40 mag) in V, 2.57 mag (14.08 to 16.65 mag) in R and 3.13 mag (13.12 to 16.25 mag) in I band). From the I band observations, we found the faintest state of the source $I = 17.45 \pm 0.05$ on April 28, 1997. Therefore, a variation of 4.33 mag (13.12 to 17.45 mag) was found in I band during the period of 1997 to 2002. Our observations presented in Table 2 indicate the source to be variable with the variability parameter C being $C_V = 6.22$, $C_R = 12.5$, and $C_I = 5.92$ for V, R and I bands respectively. We found micro-variability in the source on Jan. 25, 1998 (JD 2450839), 4σ variation of 0.3 mag in 1 hour in V band and 12σ variation of 0.48 mag over 80 minutes in I band.

3. Long-term optical photometry data

4C 29.45 is an important blazar and was often observed by different groups. We compiled the optical data of the source from the available literature (Ghosh et al. 2000; Glassgold et al. 1983; Katajainen et al. 2000; Mead et al. 1990; Raiteri et al. 1999; Sitko et al. 1982; Sitko & Sitko 1991; Smith et al. 1987; Smith et al. 1988; Villata et al. 1997; Webb et al. 1988; Wills et al. 1983; Xie et al. 1994) and our observations. The data points from the literature are listed in Table 3, which shows clearly that most of observations are from the papers by Raiteri et al. (1999), Villata et al. (1997), Webb et al. (1988), and Wills et al. (1983). The data in the papers by Raiteri et al. (1999) and Villata et al. (1997) are given in the stan-

dard B, V (Johnson), and R (Cousins) bands. In Webb et al. (1988), the U, B, and V data are in the standard Johnson UB system, they listed 145 B data for 4C 29.45. For the data given in Wills et al. (1983), we compared some of them with those in Webb et al. (1988). We chose those values given in the two literatures are quite consistent and that there is no system difference. For data given in Glassgold et al. (1983), we compared those data that have the same observation time with those in Wills et al. (1983) and found that those values given in the two literatures are quite consistent. The data given in Raiteri et al. (1998) and Villata et al. (1997) are in the same system and there is no system difference. We also compared the data by Katajainen et al. (2000) with those by Raiteri et al. (1999), and found that there is no clear difference for those data with the similar observation time. The data given by our monitoring programme are also in standard Johnson and Cousins system. Therefore, the data compiled in this paper are in the same passband system, there are no large system errors amongst the data. Some papers reported flux densities which were converted to magnitudes by using the original magnitude-flux density formula. No de-reddening correction was applied for the high galactic latitude ($b^{II} = 80^\circ$) of the object. We K-corrected all the magnitudes using the formula

$$m = m^{ob} + 2.5(1 - \alpha) \log(1 + z) \quad (3)$$

where m and m^{ob} are the magnitudes, in the source and the observer frames, redshift $z = 0.729$ for 4C 29.45, and α the spectral index ($f_\nu \propto \nu^{-\alpha}$), here $\alpha = 1.7$ was adopted from Fan & Lin (1996).

The historical light curve covers a time span of 95 years (1907-2002). The data before 1974 are very sparse (Wills et al. 1983), the post 1974 early photometric observations were made in UBVR pass bands, but very recent observations were mainly made in VRI pass bands. The historical light curves were also shown by other authors (Raiteri et al. 1999; Reith & Martin 2001). Since the data before 1974 are very sparse, in our following analysis, we only consider the post-1974 UBVR data as shown in Fig. 2, which covers about 28 years (1974 to 2002).

The long-term photometric data of 4C 29.45 show the maximum UBVR variations in the source-frame are as follows: $\Delta U = 4^m.41$ (17.08 – 12.67), $\Delta B = 5^m.55$ (18.28 – 12.73), $\Delta V = 4^m.53$ (17.38 – 12.85), $\Delta R = 5^m.80$ (18.04 – 12.24), and $\Delta I = 5^m.34$ (17.03 – 11.69). We also determined the color indices from the compiled data and calculated the average color index values. They are $U - B =$

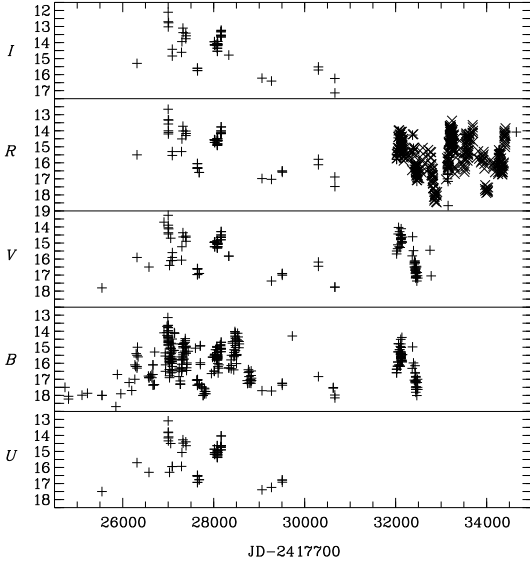


Fig. 2. Light curve of 4C 29.45. From the bottom to the top, the panels show the UBVRI light curves respectively. The crosses in R light curve represent the data from figures.

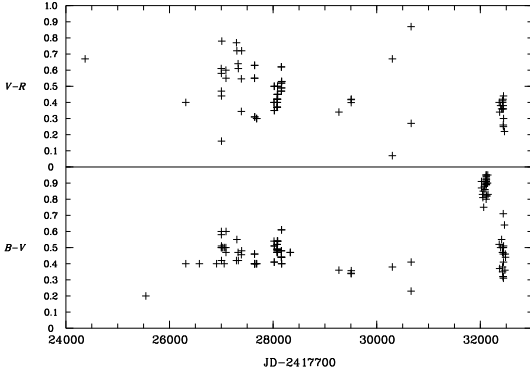


Fig. 3. Color variation. Upper panel for V-R, lower panel for B-V.

-0.54 ± 0.18 , $B - V = 0.56 \pm 0.21$, $B - R = 0.93 \pm 0.18$, $B - I = 1.51 \pm 0.24$, $V - R = 0.44 \pm 0.15$, $V - I = 1.03 \pm 0.23$ and $R - I = 0.55 \pm 0.13$. The color index variation for V-R and B-V are presented in Fig. 3 for illustration.

The available data have also shown strong correlation between R and B (and V) band data.

$$R = (1.01 \pm 3.7 \times 10^{-4})V - 0.65 \pm 8.34 \times 10^{-2},$$

$$R = (1.06 \pm 3.4 \times 10^{-4})B - 1.92 \pm 9.0 \times 10^{-2}.$$

with the correlation coefficients being 0.989.

4. Periodicity analysis

The light curves gave us an opportunity to analyze the periodicity in the light curve. As we discussed, for the data compiled in this paper there is no large system error, which will not affect the long-term periodicity analysis result. Since most data are available in R band, we only used R fluxes for the periodicity analysis. Firstly, we con-

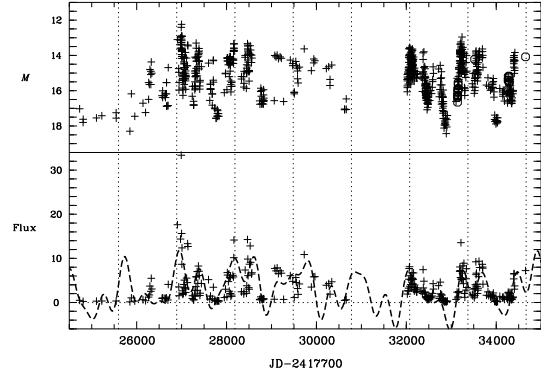


Fig. 4. R light curves. The upper panel shows the magnitude light curve, the pluses indicate the data from available literature while the open circles our observations; the lower panel the 5-day averaged R flux density (in units of mJy) light curve, the number of 5-day averaged data sample is 326. The dashed curve is the theoretical result obtained by using the two strongest CLEANest periods (Tab 4), the vertical dashed lines mean the intervals at 3.55 years.

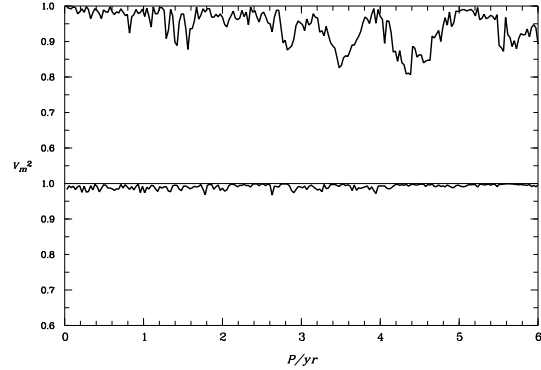


Fig. 5. Jurkevich analysis result. The upper panel is from the post-1974 light curve with $m = 5$ while the lower panel is from the re-distribution of the post-1974 light curve.

verted magnitudes to fluxes by using the magnitude-flux density formula. Secondly, in order to get nearly evenly sampled data, we averaged the flux into 5 days intervals and plotted the averaged light curve in the Fig. 4. The upper panel shows the R light curve (in magnitude), the lower panel shows the 5-day averaged light curve (in flux in units of mJy), the number of 5-day averaged data sample is 326. The 5 days interval is short enough in comparing to the long-term periods (in years) and thus unlikely to distort much the long-term variation behavior. In the following section, we will adopt Jurkevich method and power spectral analysis to the averaged R data for periodicity analysis.

4.1. Jurkevich method

The Jurkevich method (Jurkevich 1971) is based on the expected mean square deviation, it does not require an evenly distributed data sample. So, it is less inclined to generate spurious periodicity than the Fourier analysis. It tests a run of trial periods around which the data are

folded. All data are assigned to m groups according to their phases around each trial period. The variance V_i^2 for each group and the sum V_{Sm}^2 of all groups are computed. For the whole data, one can calculate the variance V_h^2 . By virtue of the well known theorem on the addition variance, Jurkevich (1971) obtained that $V_h^2 > V_{Sm}^2$. We can then get the normalization $V_m^2 = \frac{V_{Sm}^2}{V_h^2}$. If a trial period equals the true one, then V_m^2 reaches its minimum. So, a “good” period will give a much reduced variance relative to those given by other false trial periods and with almost constant values. The computation of the variances has been described in the paper of Jurkevich (1971).

Kidger et al. (1992) introduced a fraction of the variance

$$f = \frac{1 - V_m^2}{V_m^2} \quad (4)$$

where V_m^2 is the normalized value. In the normalized plot, a value of $V_m^2 = 1$ means $f=0$ and hence there is no periodicity at all. The best periods can be identified from the plot: a value of $f \geq 0.5$ suggests that there is a very strong periodicity and a value of $f < 0.25$ suggests that the periodicity, if genuine, is a weak one. A further test is the relationship between the depth of the minimum and the noise in the “flat” section of the V_m^2 curve close to the adopted period. If the absolute value of the relative change of the minimum to the “flat” section is large enough as compared with the standard error of this “flat” section, the periodicity in the data can be considered as significant and the minimum as highly reliable (Kidger et al. 1992). Here we consider the half width at half minimum as the “formal” error as done by Jurkevich (1971).

It is possible that the distribution of the measurements, particularly for the data concentrating in groups can give spurious periods, which are equal to the interval of the time of the data groups. So, it is necessary to rule out the spurious period detection. To do so, we used the Monte Carlo method to produce synthetic “measurements” and then adopted the Jurkevich method to the synthetic “measurements”. If the trial period obtained from the true measurements is also presented in the results obtained from the synthetic “measurements”, then the period is likely caused by the distribution and should be discarded. By comparing the periods obtained from the real measurements and those from the synthetic “measurements”, we can rule out the spurious periods caused by the data distributions. Therefore, the time for the synthetic “measurements” should be the same as that of the true observations. The “measurements” are produced as follows: the observing time is taken as the time of each synthetic “measurement” while the “measurements” are then chosen arbitrarily from the observed range of the actual observed data. Namely, the synthetic “measurement” is simply a random re-distribution of the actual observed data.

When the Jurkevich method was applied to the post-1974 averaged R fluxes ($m = 5$ was adopted in our analysis), we found possible periods of $P_1 = 0.82 \pm 0.03$ ($V_m^2 = 0.92$, $f = 0.08$), $P_2 = 1.43 \pm 0.15$ ($V_m^2 = 0.89$, $f = 0.12$), $P_3 = 2.82 \pm 0.07$ ($V_m^2 = 0.85$, $f = 0.17$), $P_4 = 3.48 \pm 0.16$ (V_m^2

$= 0.81$, $f = 0.23$), $P_5 = 4.38 \pm 0.12$ ($V_m^2 = 0.80$, $f = 0.25$) years. Here the selection of P2 is from the three minima covering the interval from 1.35 to 1.6 years (see Fig. 5).

When we adopted the Jurkevich method to the random re-distribution of the actual observed data for 4C 29.45, the result is shown in the lower panel in Fig. 5. By comparing the analysis results from the true and the synthetic “measurements”, we saw that all the periods appeared in the upper panel in Fig. 5 are not from the data distribution and should be possible periods.

4.2. Power spectral (Fourier) analysis

We also performed a power spectral (Fourier) analysis, because it is a powerful and common (well-studied) method to detect a periodic signal, and gives some quantitative criterion for the detection of a periodic signal.

In the case that the data are unevenly spaced in time, many attempts of power spectral analysis have been made. In widespread use by astronomers is the *modified periodogram* (Scargle 1982; Horne & Baliunas 1986), which is based on a least squares regression onto the two trial functions, $\sin(\omega t)$ and $\cos(\omega t)$. A superior technique is the *Date-Compensated Discrete Fourier Transform*, or DCDFT (Ferraz-Mello 1981; Foster 1995), a least-squares regression on $\sin(\omega t)$, $\cos(\omega t)$ and constant. The DCDFT is a more powerful method than the *modified periodogram* for unevenly spaced data, we adopted it to the R light curve, it can be done as Foster (1995) described.

The observed data $x(t_i)$ can define the data vector

$$|x\rangle = [x(t_1), x(t_2), \dots, x(t_N)]. \quad (5)$$

First, defining the *inner product* of two vectors f and g as the average value of the product f^*g over the observation times $\{t_n\}$,

$$\langle f|g\rangle = \left(\frac{1}{N}\right) \sum_{n=1}^N f^*(t_n)g(t_n) \quad (6)$$

A subspace are spanned by 3 trial functions $\phi_1(t) = 1$ (constant), $\phi_2(t) = \sin(\omega t)$ and $\phi_3(t) = \cos(\omega t)$. These 3 trial functions define a set of trial vectors,

$$|\phi_\alpha\rangle = [\phi_\alpha(t_1), \phi_\alpha(t_2), \dots, \phi_\alpha(t_N)], \quad \alpha = 1, 2, 3. \quad (7)$$

The data vector $|x\rangle$ can be projected onto the subspace spanned by the $|\phi_\alpha\rangle$ results in a model vector $|y\rangle$ and a residual vector $|\Theta\rangle$.

$$|x\rangle = |y\rangle + |\Theta\rangle \quad (8)$$

The model vector $|y\rangle$ is defined,

$$|y\rangle = \sum_{\alpha} c_{\alpha} |\phi_{\alpha}\rangle \quad (9)$$

The c_{α} can be obtained, taking the inner product of each trial vector ϕ_{α} with the data vector x , we have

$$\langle \phi_{\alpha}|x\rangle = \sum_{\beta} c_{\beta} \langle \phi_{\alpha}|\phi_{\beta}\rangle = \sum_{\beta} S_{\alpha\beta} c_{\beta}, \quad (10)$$

which defines the S matrix $S_{\alpha\beta}$. Inverting this matrix yields the coefficients,

$$c_\alpha = \sum_{\beta} S_{\alpha\beta}^{-1} \langle \phi_\beta | x \rangle \quad (11)$$

s^2 is the estimated data variance, it can be replaced by σ^2 . The power level of DCDFT is,

$$P_X(\omega) = \frac{1}{2} N [\langle y|y \rangle - \langle 1|y \rangle^2] / s^2 \quad (12)$$

We adopted the *False Alarm Probability*, *FAP* (Horne & Baliunas 1986), to give an a quantitative criterion for the detection of a periodic signal derived by DCDFT. Horne & Baliunas (1986) introduced the False Alarm Probability to deal with the modified periodogram. In fact, the False Alarm Probability (FAP) can deal with all kinds of Fourier analysis method if the variations (mainly) consist of randomly distributed noise. In Fig 6 and 7 we noticed that the noise is almost randomly distributed. It has been done by steps described here.

First, the power level of the periodogram is normalized by the total variance σ ,

$$P_N(\omega) = P_X(\omega) / \sigma^2 \quad (13)$$

The probability that $P_N(\omega_0)$ is of height z or higher is $Pr[P_N(\omega_0) > z] = e^{-z}$. Suppose that z is the highest peak in a periodogram that sampled N_i independent frequencies. The probability that each independent frequency is smaller than z is $1 - e^{-z}$, so the probability that every frequency is lower than z is $[1 - e^{-z}]^{N_i}$. Thus, the false alarm probability can be defined,

$$FAP = 1 - [1 - e^{-z}]^{N_i} \quad (14)$$

For the independent frequencies, N_i , it is not too difficult to obtain N_i by simple Monte Carlo, and the estimate of N_i is not need be very accurate (Press et al. 1994). We adopted $N_i = N_0/2.9$ in the case of our unevenly sampled data, $N_0 = 326$ is the scale of our 5-day averaged data sample.

The DCDFT power spectral analysis are applied to the post-1974 averaged R data and the re-distributed observation data, the resulting DCDFT is shown in Fig. 6. The upper panel is from the actual data while the lower panel is from the re-distribution of the actual observed data. In the periodogram, various false alarm probability levels are marked. The highest peak is at $T = 3.44 \pm 0.24$ years, with a false probability of $FAP = 0.136$. The second one is at $T = 4.43 \pm 0.28$ years, with a false probability of $FAP = 0.233$, the third one is at $T = 1.42 \pm 0.05$ years, with a false probability of $FAP = 0.326$. The false probabilities of other peaks are all higher than 0.50.

4.3. CLEANest analysis

In the case of unevenly sampled time series analysis, irregular spacing introduces myriad complications into the Fourier transform. It can alter the peak frequency (slightly) and amplitude (greatly), even introduce extremely large false peaks.

Foster (1995) proposed the CLEANest analysis to clean false periodicities, we also tried to do the CLEANest analysis. the CLEANest algorithm can remove false peaks. First, the strongest single peak and corresponding false

components are subtracted first from the original spectrum, then the residual spectrum is scanned to determine whether the strongest remaining peak is statistically significant. If so, then the original data are analyzed to find the pair of frequencies which best models the data, these 2 peaks and corresponding false components are subtracted, and the residual spectrum is scanned. The process continues, producing CLEANest spectrum, until all statistically significant frequencies are included. We assume that there are 7 independent frequency components to clean observation data, the CLEANest spectrum is shown in Fig 7, and the results listed in Tab. 4.

The variance of a frequency $Var(\omega)$ and the variance of the amplitude of the given frequency $Var(P)$ can be estimated by Foster (1996)

$$Var(\omega) = \frac{24\sigma_{res}^2}{NA^2T^2} \quad (15)$$

$$Var(P) = \frac{2\sigma_{res}^2}{N} \quad (16)$$

where σ_{res} is the variance of the residual data, A is the amplitude of the given frequency and T is the total time span. The σ_{res}^2 is estimated by

$$\sigma_{res}^2 = \frac{NV_{res}}{N - 3f - 1}, \quad (17)$$

where V_{res} is the variance of residual data, $V_{res} = \langle res|res \rangle - \langle 1|res \rangle$, and f is the number of discrete frequencies.

We also introduce the False Alarm Probability to deal with CLEANest frequency components, because of the same definition of amplitude. *FAP* are also listed in Tab 4, the strongest component at $T = 3.55 \pm 0.02$ years, with a amplitude 6.87 ± 0.63 and with a false probability of $FAP = 0.11$, the second one at $T = 1.58 \pm 0.01$ years, with a amplitude 5.21 ± 0.63 and with a false probability of $FAP = 0.46$. The false probabilities of other components and residual spectrum are more higher than 0.50. Notably, FAP means a strong enough signal with a small probability to be false, for a weak signal with stronger signal, it is can be true but with a large FAP.

4.4. Periodicity analysis results

We listed periodicity analysis results derived by JV method, DCDFT and CLEANest in Tab 5. Jurkevich method gives 5 possible periods, a closer look at all these 5 possible periods showed that $P_3 \sim 2P_2$. Therefore, P_3 are harmonics of the P_2 , so P_2 is a possible period along with P_1 , P_4 and P_5 . From power spectral (Fourier) analysis, we got 3 possible periods at 3.44 years ($\sim P_4$), 4.43 years ($\sim P_5$) and 1.42 years ($\sim P_2$), with false alarm probabilities lower than 0.40. Using two different analysis methods, we got the same results. These signals may be influenced by irregular spacing, the peak frequencies and amplitudes are altered some. From CLEANest analysis, we correct the influence and derived 2 periods at 3.55 ($\sim P_4$) years and 1.58 ($\sim P_2$) years, with FAPs lower than 0.50 and amplitudes more than three times variance. So, we could conclude that there are two possible periods of 1.58 and

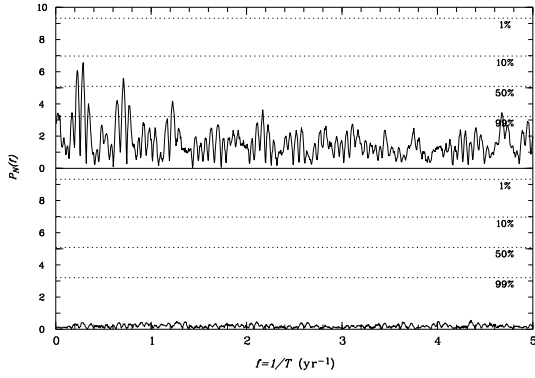


Fig. 6. The normalized Fourier analysis result for R light curve. The upper panel is from the post-1974 light curve while the lower panel is from the re-distribution of the same light curve. In the upper panel, the highest peak is at $T = 3.44 \pm 0.24$ years, with a false probability of $FAP = 0.136$, various false alarm probability levels are marked.

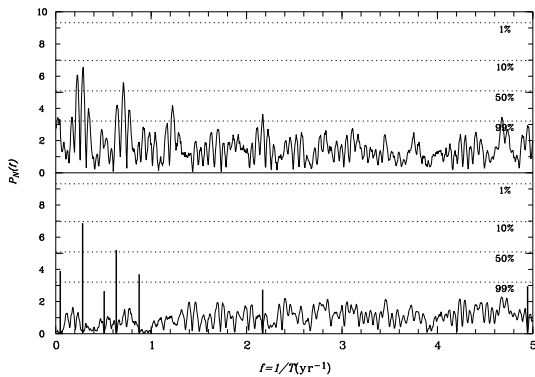


Fig. 7. The Fourier analysis and the CLEANest spectrum for R light curve. The upper panel is the Fourier analysis from the post-1974 light curve while the lower panel is the CLEANest spectrum from the same light curve. In the lower panel, 7 CLEANest frequency components (rough lines) and the residual spectrum are shown. Various false alarm probability levels are marked.

3.55 years. We marked the light curve using the interval of 3.55 years, and showed the theoretical light curve obtained by using the two strongest CLEANest periods (3.55 and 1.58 years) (see Tab 4) in Fig 4.

5. Optical and Radio Correlation

4C 29.45 is also variable in the radio bands, light curves covering the period from 1980 to 2002 were shown by Hong et al. (2004). It shows clear outbursts at the radio and optical bands as shown in Fig. 8. Is there any correlation between the radio and optical variation for the source? To study this, we adopted the discrete correlation function (DCF) method to the radio and the optical data. The DCF method, which was described in detail by Edelson & Krolik (1988) (Fan et al. 1998b), is intended for analysis of the correlation of two data sets. This method can indicate the correlation of two variable temporal series with a time

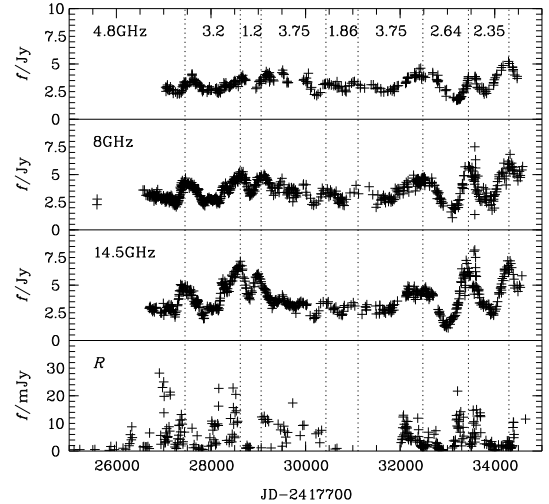


Fig. 8. Radio and optical light curves. The panels from the top to the bottom are the 4.8GHz radio light curve, 8GHz light curve, 14.5GHz light curve and optical R light curve.

lag. It can be done as follows.

Firstly, we have calculated the set of unbinned correlation (UDCF) between data points in the radio and optical data streams a (for the optical data) and b (for the radio data), i.e.

$$UDCF_{ij} = \frac{(a_i - \bar{a}) \times (b_j - \bar{b})}{\sqrt{\sigma_a^2 \times \sigma_b^2}}, \quad (18)$$

where a_i and b_j are points in the data sets, \bar{a} and \bar{b} are the average values of the data sets, and σ_a and σ_b are the corresponding standard deviations. Secondly, we have averaged the points sharing the same time lag by binning the $UDCF_{ij}$ in the suitable sized time-bins in order to get the DCF for each time lag τ :

$$DCF(\tau) = \frac{1}{M} \sum UDCF_{ij}(\tau), \quad (19)$$

where M is the total number of pairs. The standard error for each bin is

$$\sigma(\tau) = \frac{1}{M-1} \{ \sum [UDCF_{ij} - DCF(\tau)]^2 \}^{0.5}. \quad (20)$$

When Eqs. (18) to (20) are applied to the post-1974 optical R and the radio data as shown in Fig. 8, the resulting DCF result is obtained and shown in Fig. 9. For the optical and the radio variation, there is a very weak correlation with the optical variation leading the 14.5GHz radio variation by 520–560 days. For comparison, the DCF results for radio bands are also calculated and shown in Fig. 9. For the radio band light curves, there is clear correlation between the 14.5 GHz light curve and the 8.0GHz as well as the 8.0GHz light curves with the 4.8GHz variation leading the 4.8GHz by about 0 ~ 280 days.

6. Discussion and conclusion

The compiled data of the OVV 4C 29.45 indicate large optical flux variations. From our observations, we found a

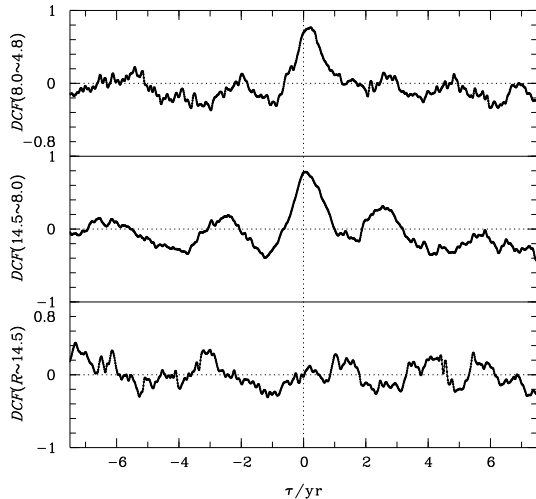


Fig. 9. DCF result for the post-1974 data. The top panel is for the 8.0 GHz and the 4.8GHz radio data, the middle one for the 14.5GHz and 8GHz data, the bottom panel for the DCF result between optical R data and the 14.5GHz radio data (DCF bin: 30 days).

faint state of the source $I = 17.45 \pm 0.05$ on April 28, 1997. Xie et al. (1994) also reported a faint state of the source $I = 17.14$ in their observations in 1991. Our data show that the source was even 0.3 mag fainter in I in 1997 compared to 1991. In addition, Villate et al. (1999) monitored the source during the period of January 04, 1995 to May 27, 1998 and found a variation of 5.1 mag. The faintest state of the source was detected by them on May 21, 1997 ($R = 18.46$). Present observations and observations by Villate et al. (1999) show that the source was in a low-state in the first half of the year 1997.

For periodicity analysis, according to a paper by Kidger et al. (1992), we found that all the periods determined from Jurkevich method are weak. Further consideration indicated that the physically possible periodicity is P_1 , P_2 , P_4 and P_5 . When the power spectral (Fourier) analysis is adopted to the R flux, the analysis result clearly shows that there are three possible periods at 3.44 years, 4.43 years and 1.42 years, with false alarm probabilities being smaller than 0.40. When we used the CLEANest analysis to correct the influence of irregular spacing, we obtained two corresponding periods at 3.55 years and 1.58 years.

For comparison, we also used the DCF method for periodicity analysis as we did in our previous paper (Fan et al. 2002), and found period signs at 3.2 ± 0.08 and 4.15 ± 0.15 years. However, there is no sign of 1.4 or 1.6 year period in the analysis result obtained by DCF method. For the DCF method itself, we found that it is a powerful periodicity analysis method if there is only one period in the light curve. However, if more than one period is present, DCF analysis will dilute the sign of other periods. Therefore, DCF is an excellent method for single period analysis but for multiple periods. We think that the DCF analysis result should be compared with other methods.

It is interesting that its infrared light curves also show an interval of 3.2 years in our previous work (Fan 1999a), which is marginally consistent with the 3.55 ± 0.1 years period. So, we can say that there are two possible periods of 1.58 and 3.55 years in the light curve.

There are some popular models which can explain the long-term periodic variations in AGNs viz. Double black hole model, the thermal instability model, and the perturbation model (Sillanpää et al. 1988; Meyer & Meyer-Hofmeister 1984; Abraham & Romero 1999; Romero et al. 2003; Rieger 2004; Xie et al. 2004; Wu et al. 2005).

The thermal instability of slim accretion disk is a suitable model to see the long term variability behavior. This model can explain ultra-short period variable with a shorter duration of quiescence phase. Periodicity time scale of a few years can not be produced by the thermal instabilities (Fan 1999b). Variability behavior of 4C 29.45 reported here has shown the time scale of a few years which can not be supported by the model. So, this model is ruled out for the explanation for the present work.

The perturbation model based on the accretion disk pulsations, the presence of a single dominant hot spot on the disk. The model can show the periodicity in blazar on timescales of a week or less. Here we reported the periodicity of the time scale of a few years which can not be supported by this model.

Sillanpää et al. (1988) suggested a double black hole model for the blazar and predicted that the outburst in the blazar OJ 287 should occur in 1994. The predicted outburst was really observed in their OJ-94 project Sillanpää et al. (1996). The model given by Sillanpää et al. (1988) is a well established model for the long term periodic variation and the prediction of next outburst in blazars. The periodicity reported here can be successfully explained by the model.

4C 29.45 shows variation in the radio as well as in the optical band, the variations in the two bands show weak correlation with the optical variation leading the 8GHz radio one by 520-560 days. The variations at the three frequencies (4.8GHz, 8GHz, and 14.5 GHz) are correlated with the variations at higher frequencies leading the ones at lower frequencies.

In the present paper, we reported our optical (VRI) monitoring results for the blazar 4C 29.45 during the period of 1997 to 2002. The historic data were also compiled from the available literature. The data presented in the paper showed that the source shows large variations in UBVRI bands. In addition, we adopted the periodicity analysis methods to the R band light curve and found that there are possible variation periods of 1.58 and 3.55 years.

We thank the referee for the constructive comments and suggestions, and Dr. V. R. Chitnis for correcting English of the paper. This work is partially supported by the National 973 project (NKBRFSF G19990754), the National Science Fund for Distinguished Young Scholars (10125313), the National Natural Science Foundation of China (10573005), and the Fund for Top Scholars of Guangdong Province (Q02114). We also thank the finan-

cial support from the Guangzhou Education Bureau and Guangzhou Science and Technology Bureau. ACG's efforts are partially supported by the Department of Atomic Energy, Govt. of India.

References

- Abraham, Z., Romero, G. E., 1999, *A&A*, 344, 61
- Branly, R., Kilgard, R., Sadun, A., Shcherbanovskiy, A., Webb J. 1996, *ASP Conf. Ser. Vol. 110*, p170
- Cellone, S. A., Romero, G. E., Combi, J. A., 2000, *AJ*, 119, 1534
- Ciprini, S., Tosti, G., Raiteri, C. M., Villata, M., Ibrahimov, M. A., Nucciarelli, G., Lanteri, L., 2003, *A&A*, 400, 487
- Ciprini, S., Tosti, G., Teräsraanta, H., Aller, D., 2004, *MNRAS*, 348, 1379
- Clements, S. D., Jenks, A., Torres, Y., 2003, *AJ*, 126, 37
- Edelson, R. A., Krolik, J. H., 1988, *ApJ*, 333, 646
- Fan, J. H., 2005, *ChJA&A*, 5S, 213
- Fan, J. H., Lin, R. G., Xie, G.Z., et al. 2002, *A&A*, 381, 1
- Fan, J. H., Qian, B. C., Tao, J., 2001, *A&A*, 369, 758
- Fan, J.H., 1999a, *MNRAS*, 308, 1032
- Fan, J.H., 1999b, *A&A*, 347, 419
- Fan, J. H., Xie, G. Z., Pecontal, E., et al. 1998a, *ApJ* 507, 178
- Fan, J. H., Xie, G. Z., Lin, R. G., et al. 1998b, *A&AS*, 133, 217
- Fan, J. H., Xie, G. Z., Lin, R. G., et al. 1997, *A&AS*, 125, 525
- Fan, J.H., & Lin R.G., 1996, *YunO*. 65, 8
- Ferraz-Mello, S, 1981, *AJ*, 86, 619
- Fiorucci, M., Ciprini, S., Tosti, G., 2004, *A&A*, 419, 25
- Foster, G. 1996, *AJ*, 111, 541
- Foster, G. 1995, *AJ*, 109, 1889
- Ghosh, K. K., Ramsey, B. D., Sadun, A. C., Soundararajaperumal, S., 2000, *ApJS*, 127, 11
- Glassgold, A. E., Bergman, J. M, Huggins, P. J., et al., 1983, *ApJ*, 274, 101
- Gu, M.F., Lee1, C.-U., Pak1,S., Yim1, H. S. , Fletcher, A. B. 2006, *A&A*, (accepted)(astro-ph/0602180)
- Holmes, P. A., Brand, P. W. J. L, Impey, C. D., Williams, P. M., 1984, *MNRAS*, 210, 961
- Hong, X. Y., Jiang, D. R., Gurvits, L. I., Garrett, M. A., Garrington, S. T., Schilizzi, R. T., Nan,R. D., Hirabayashi, H., Wang,W. H., and Nicolson, G. D., 2004, *A&A*, 417, 887
- Hong, X. Y., Jiang, D. R, Gurvits L.I., et al. 1999, *NewAR*, 43, 699
- Horne, J., & Baliunas, S. 1986, *ApJ*, 302, 757
- Jurkevich I., 1971, *Ap&SS*, 13, 154
- Katajainen, S., Takalo, L., Sillanpää, A., et al. 2000, *A&AS*, 143, 357
- Kidger, M. R., Takalo, L., Sillanpää, A. 1992, *A&A* 264, 32
- Lainela, M., Takalo, L. O., Sillanpää, A., et al. 1999, *ApJ*, 521, 561
- Liu, F. K., Xie, G. Z., 1995, *A&A*, 295, 1
- Manchanda, K. R., 2002, *JApA*, 23, 243
- Mead, A. R. G., Ballard, K. R., Brand, P. W. J. L., et al. 1990, *A&AS*, 83, 183
- Meyer, F., Meyer-Hofmeister, E. 1984, *A&A*, 132, 143
- Noble, J. C, Miller, H. R., 1996, *ASP Conf. Ser. 110*, p30
- Press, H. W., Teukolsky, A. S., Vetterling, T. W., & Flannery, P. B., *Numerical Recipes in Fortran –The art of scientific computing*, second edition, p569
- Qian, B.-C., Tao, J., 2004, *PASP*, 116, 161
- Qian, B.-C., Tao, J., Fan, J.H., 2004, *PASP*, 116, 634
- Raiteri, C. M., Villata, M., Aller, H. D., et al. 2001, *A&A*, 377, 396
- Raiteri, C. M., Villata, M., Balonek, T. J., et al. 1999, *OJ-94 Annual Meeting 1999, Torino* , 19-21 May 1999, blazar monitoring, Eds, C.M., Raiteri, M., Villata, L.O., Takalo. p79
- Raiteri, C. M., Ghisellini, G., Villata, M., et al. 1998, *A&AS*, 127, 445
- Reith, C. N., Martin J. G., 2001, *usra.proc*, eds, K. B. Kwitter, P. J. Benson, p113
- Rieger, F., 2004, *ApJL*, 615, L5
- Romero, G.E., Cellone, S.A., Combi J.A., 1999, *A&AS*, 135, 477
- Romero, G., Fan J.H., Nuza, S.E., 2003, *ChJAA*, Vol. 3, 513
- Scargle, J. 1982, *ApJ*, 263, 835
- Sillanpää, A., Haarala, S., Valtoneni, M. J., et al. 1988, *ApJ*, 325, 628
- Sillanpää, A., Takalo L. O., Pursimo, T., et al. 1996, *A&A*, 305, L17
- Sitko, M. L., Sitko, A. K. 1991, *PASP* 103, 160
- Sitko, M. L., Stein, W. A., Zhang, Y. X., Wisniewski, W. Z., 1982, *ApJ*, 259, 486
- Smith, P. S., Balonek, T., Heckert, P., Elston, R., Schmidt, G. D., 1985, *AJ*, 90, 1184
- Smith, P. S., Balonek, T., Elston, R., et al. 1987, *ApJS*, 64, 459
- Smith, P. S., Elston, R., Berriman, G., et al. 1988, *ApJ*, 326, 39
- Urry, C. M. & Padovani, P., 1995, *PASP*, 107, 803
- Villata, M., Raiteri, C. M., Balonek, T.J., et al. 1999, *BL Lac Phenomenon, ASP Conf. Series Vol. 159*, Eds. L.O. Takalo and A. Sillanpää, p107.
- Villata, M., Raiteri, C. M., Ghisellini, G., et al. 1997, *A&AS*, 121, 119
- Webb, J. R., Smith, A. G., Leacock, R. J., et al. 1988, *AJ*, 95, 374
- Wills, B. J., Pollock, J. T., Aller, H. D., et al, 1992, *ApJ*, 398, 454
- Wills, B. J., Pollock, J. T., Aller, H. D., et al, 1983, *ApJ*, 274, 62
- Wu, J. H. et al. 2005, *MNRAS*, 361, 155
- Xie, G. Z., Li, K. H., Zhang, Y. H., et al. 1994, *A&AS*, 106, 361
- Xie, G. Z., Zhou, S. B., Li, K. H., et al. 2004, *MNRAS*, 348, 831
- Zhang, X., Xie, G. Z., Bai, J. M., 1999, *ChA&A*, 23, 272

Table 2. Observational Journal for 4C 29.45

<i>JDdate</i>	V	σ_V	R	σ_R	I	σ_I
(1)	(2)	(3)	(4)	(5)	(6)	(7)
2450567.118					17.45	0.04
2450567.121					17.05	0.05
2450567.15					17.27	0.15
2450839.297					15.95	0.05
2450839.309	16.80	0.07				
2450839.316					15.77	0.05
2450839.326	16.90	0.07				
2450839.331					16.02	0.05
2450839.335			16.28	0.03		
2450839.339	17.12	0.07				
2450839.348					15.99	0.05
2450839.353			16.36	0.03		
2450839.362					15.91	0.05
2450839.366			16.38	0.03		
2450839.37	17.01	0.07				
2450839.374					16.25	0.05
2450839.378			16.65	0.03		
2450839.382	16.82	0.07				
2450843.263					15.72	0.01
2450843.269			16.25	0.06		
2450843.28	16.21	0.09				
2450843.289					15.47	0.01
2450843.293			15.93	0.06		
2450843.306	16.79	0.09				
2450843.314					15.73	0.01
2450843.319			16.28	0.06		
2450843.342			16.06	0.06		
2450843.347	16.64	0.09				
2450853.196					15.51	0.08
2450853.201			15.67	0.1		
2450853.212					15.39	0.08
2450853.229					16.00	0.08
2450853.239	16.22	0.18				
2450853.245					15.62	0.08
2450853.249			15.55	0.1		
2450853.262	16.35	0.18				
2450853.272					15.72	0.08
2450853.3					15.40	0.08
2450853.305			15.96	0.1		
2450853.311	16.40	0.18				
2450853.322			15.88	0.1		
2450853.327	16.26	0.18				
2450853.332					15.33	0.08
2450853.336			15.91	0.1		
2450853.341	16.33	0.18				
2451219.199					13.12	0.01
2451219.208					13.65	0.01
2451219.235			14.23	0.02		
2451229.246	16.21	0.05				
2451254.189					14.67	0.23
2451254.199			15.11	0.26		
2451254.207	15.32	0.24				
2451913.357					16.15	0.27
2451955.223					15.74	0.18
2451955.233					15.86	0.05

Table 2. (Continued)

<i>JDdate</i>	V	σ_V	R	σ_R	I	σ_I
(1)	(2)	(3)	(4)	(5)	(6)	(7)
2451955.291	16.60	0.15				
2451959.139					15.91	0.27
2451959.156					15.72	0.29
2451959.164					15.54	0.30
2451959.172			16.05	0.01		
2451959.187			15.94	0.01		
2451965.129					14.45	0.15
2451965.141			15.21	0.07		
2451965.168	15.86	0.28				
2451965.187			15.43	0.07		
2451965.198					14.45	0.11
2451965.203			15.40	0.07		
2451965.211	16.69	0.05				
2451986.152					14.53	0.05
2451986.157					14.74	0.05
2451986.206			15.27	0.05		
2451986.217			15.48	0.07		
2451986.23			15.20	0.05		
2451986.254			15.17	0.05		
2451990.126					15.15	0.15
2451990.127			15.53	0.05		
2451990.14	16.08	0.05				
2451990.153					14.96	0.15
2451990.158			15.56	0.05		
2452352.148			14.08	0.12		

Table 3. Data Base (points) for 4C 29.45

Author (1)	Time(UT/JD) (2)	U (3)	B (4)	V (5)	R (6)	I (7)	Note (8)
Glassgold et al. (1983)	1982 04 28 2445087.135	1	2	2	2	2	flux
Mead et al. (1990)	1988 02 15–1988 02 17 2447206.348–2447208.348	3	3	3	2		flux
Katajainen et al. (2000)	1996 01 26–1997 02 01 2450108.554–2450480.479			11			mag
Present Work	1998 01 25–2002 02 18 2450839.302–2452352.148				32		mag
Raiteri et al. (1999)	1995 01 04–1996 04 13 2449721.609–2450186.383		56	48	15		mag
Smith et al. (1987)	1983 01 08–1984 06 14 24453342.5–2445865.5	20	20	20	20	18	mag
Villata et al. (1997)	1995 01 04–1995 05 09 2449721.608–2449847.3594				31		mag
Webb et al. (1988)	1980 05 09–1986 04 12 2444368.6–2446532.6		145				mag
Wills et al. (1983)	1907 05 06–1983 07 15 2417702–2445531.178	19	102	22	16	14	mag
Xie et al. (1994)	1990 04 20–1991 04 18 2448001.075–2448364.318		5	4	4	4	mag
Raiteri et al. (1998)	1995 05 12–1995 12 07 2451389.305–2452117.233				16		fig
Raiteri et al. (1998)	1996 04 28–1999 06 02 2450201.667–2451332.167				94		
Reith & Martin (2001)	1999 07 29–2001 07 26 2451389.305–2452117.233				78		fig
Webb et al. (1988)	1987 01 04–1990 01 28 2446800–2447920				23		fig

Table 4. Seven CLEANest frequency components for blazar 4C 29.45.

Frequency (cycles/yr)	Period (yr)	Coeff.	FAP
0.28	3.55 ± 0.02	6.87 ± 0.63	0.11
0.63	1.58 ± 0.01	5.21 ± 0.63	0.46
0.05	21.1 ± 0.51	3.90 ± 0.63	0.90
0.88	1.14 ± 0.01	3.70 ± 0.63	0.94
5.00	0.20 ± 0.01	2.96 ± 0.63	1.00
2.17	0.46 ± 0.01	2.74 ± 0.63	1.00
0.51	1.97 ± 0.01	2.66 ± 0.63	1.00

Table 5. Periodicity analysis results.

	P_1 (yr)	P_2 (yr)	P_3 (yr)	P_4 (yr)	P_5 (yr)
JV	0.82 ± 0.03	1.43 ± 0.15	2.82 ± 0.07	3.48 ± 0.16	4.38 ± 0.12
DCDFT		1.42 ± 0.05		3.44 ± 0.24	4.43 ± 0.28
CLEANest		1.58 ± 0.01		3.55 ± 0.02	